Cellular/Molecular

Interplay between Na^+/Ca^{2+} Exchangers and Mitochondria in Ca^{2+} Clearance at the Calyx of Held

Myoung-Hwan Kim,[1] Natalya Korogod,[2] Ralf Schneggenburger,[2] Won-Kyung Ho,[1] and Suk-Ho Lee[1]

[1]National Research Laboratory for Cell Physiology, Department of Physiology, Seoul National University College of Medicine, Chongno-Ku, Seoul 110-799, Korea, and [2]Arbeitsgruppe Synaptische Dynamik und Modulation and Abteilung Membranbiophysik, Max-Planck-Institut für Biophysikalische Chemie, D-37077 Göttingen, Germany

The clearance of Ca^{2+} from nerve terminals is critical for determining the build-up of residual Ca^{2+} after repetitive presynaptic activity. We found previously that K^+-dependent Na^+/Ca^{2+} exchangers (NCKXs) show polarized distributions in axon terminals of supraoptic magnocellular neurons and play a major role in Ca^{2+} clearance. The role of NCKXs in presynaptic terminals, however, has not been studied. We investigated the contribution of NCKX in conjunction with other Ca^{2+} clearance mechanisms at the calyx of Held by analyzing the decay of Ca^{2+} transients evoked by depolarizing pulses. Inhibition of Na^+/Ca^{2+} exchange by replacing external Na^+ with Li^+ decreased the Ca^{2+} decay rate by 68%. Selective inhibition of NCKX by replacing internal K^+ with TEA^+ (tetraethylammonium) or Li^+ decreased the Ca^{2+} decay rate by 42%, and the additional inhibition of the K^+-independent form of Na^+/Ca^{2+} exchanger (NCX) by reducing external $[Na^+]$ caused an additional decrease by 26%. Inhibition of plasma membrane Ca^{2+}-ATPase (PMCA) decreased the Ca^{2+} decay rate by 23%, whereas inhibition of SERCA (smooth endoplasmic reticulum Ca^{2+}-ATPase) had no effect. The contribution of mitochondria was negligible for small Ca^{2+} transients but became apparent at $[Ca^{2+}]_i > 2.5\ \mu M$, when Na^+/Ca^{2+} exchange became saturated. Mitochondrial contribution was also observed when the duration of Ca^{2+} transients was prolonged by inhibiting Na^+/Ca^{2+} exchangers or by increasing Ca^{2+} buffers. These results suggest that, in response to small Ca^{2+} transients ($<2\ \mu M$), Ca^{2+} loads are cleared from the calyx of Held by NCKX (42%), NCX (26%), and PMCA (23%), and that mitochondria participate when the Ca^{2+} load is larger or prolonged.

Key words: **presynaptic; calcium clearance; NCX; NCKX; mitochondria; calyx of Held**

Introduction

In presynaptic axon terminals, calcium plays a key role in activity-dependent changes in synaptic strength as well as for the release of neurotransmitter. Incoming Ca^{2+} during action potentials (APs) rapidly equilibrates with Ca^{2+} buffers and then decays by the concerted action of different Ca^{2+} clearance mechanisms (CCMs): plasma membrane Ca^{2+}-ATPase (PMCA), Na^+/Ca^{2+} exchanger (Na/CaX), smooth endoplasmic reticulum Ca^{2+}-ATPase (SERCA), and mitochondria. Recent studies have shown that presynaptic CCMs have a strong influence on presynaptic residual calcium, which has been proposed as an underlying mechanism for short-term synaptic plasticity. It has been reported that presynaptic residual calcium after a period of high-frequency activity is caused by Ca^{2+} influx through a reverse-mode Na/Ca exchange or by a delayed Ca^{2+} release from mitochondria subsequent to the Ca^{2+} uptake (Tang and Zucker, 1997; Zhong et al., 2001). Investigating the quantitative role of different CCMs in nerve terminals will thus provide a basic understanding of the mechanisms underlying short-term plasticity.

There is evidence for presynaptic roles of PMCA in retinal bipolar cells (Zenisek and Matthews, 2000), for Na/CaX in cultured hippocampal neurons (Reuter and Porzig, 1995) and in cerebellar granule cells (Regehr, 1997), and for mitochondria in sympathetic ganglion (Peng, 1998). Previous studies on presynaptic CCMs aimed to determine the contribution of specific mechanisms but have not provided a comprehensive picture of how different CCMs interact with each other as a function of the cytosolic $[Ca^{2+}]$ attained after a stimulus. Considering that these mechanisms have different properties in terms of the affinity and the clearance capacity for Ca^{2+}, intracellular calcium load might be one of the important factors that affect the relative contribution of CCMs (Fierro et al., 1998; Suzuki et al., 2002; Kim et al., 2003). In this respect, quantitative studies are required to elucidate the extent to which each CCM contributes depending on calcium load.

At the calyx of Held, a mammalian giant presynaptic terminal, $[Ca^{2+}]_i$ can be measured quantitatively using Ca^{2+} indicator dye introduced via a patch pipette. Recently, it has been reported that mitochondria contribute to the Ca^{2+} clearance at the calyx of Held and that mitochondrial Ca^{2+} uptake affects recovery from synaptic depression (Billups and Forsythe, 2002). However,

Received Feb. 2, 2005; revised May 13, 2005; accepted May 14, 2005.

This work was supported by Grant M103KV010012-03K2201-01220 from the Brain Research Center of the 21st Century Frontier Research Program and Grant for National Research Laboratory 2004-02433 from the Ministry of Science and Technology, Republic of Korea. M.-H.K. was a postgraduate student supported by Program BK21 from the Ministry of Education.

Correspondence should be addressed to Dr. Suk-Ho Lee, Department of Physiology, Seoul National University College of Medicine, Chongno-Ku, Yongon-Dong 28, Seoul 110-799, Korea. E-mail: leesukho@snu.ac.kr.

DOI:10.1523/JNEUROSCI.0454-05.2005

Copyright © 2005 Society for Neuroscience 0270-6474/05/256057-09$15.00/0

Chuhma and Ohmori (2002) showed that the Ca^{2+} extrusion rate was reduced by inhibition of Na/CaX at the same preparation. Functional and immunocytochemical evidence indicates the existence of Na/CaX in the presynaptic terminals of other mammalian CNS synapses (Reuter et al., 1995; Regehr, 1997). Moreover, we recently described the role of a K^+-dependent form of Na^+/Ca^{2+} exchanger (NCKX) in peptidergic axon terminals and found that its distribution is polarized to the axon terminals in hypothalamic magnocellular neurons (Lee et al., 2002; Kim et al., 2003). The role of NCKX, however, has not yet been studied in CNS presynaptic terminals, probably because of the inaccessibility of most nerve terminals for intracellular ion exchange experiments. Here, we tested whether NCKX contributes to Ca^{2+} clearance at the calyx of Held and elucidated the dependence of the relative contributions of Na/CaX and other CCMs, especially mitochondria, on the intracellular calcium load.

Materials and Methods

Preparation of brainstem slices. Transverse brainstem slices containing the medial nucleus of the trapezoid body (MNTB) were prepared from 8- to 10-d-old Sprague Dawley rats (17 ± 4 g). Rats were decapitated, and brainstems were chilled in ice-cold low-calcium artificial CSF (aCSF) containing the following (in mM): 125 NaCl, 25 $NaHCO_3$, 2.5 KCl, 1.25 NaH_2PO_4, 2.5 $MgCl_2$, 0.5 $CaCl_2$, 25 glucose, 0.4 Na ascorbate, 3 *myo*-inositol, 2 Na pyruvate, at pH 7.4, when saturated with carbogen (95% O_2, 5% CO_2), and with an osmolarity of ~320 mOsm. Isolated brainstems were glued onto the stage of a vibratome (VT1000S; Leica, Wetzlar, Germany), and 150- to 200-μm-thick transverse brainstem slices were cut from caudal to rostral in the same solution. Slices containing the MNTB (approximately four to five slices) were incubated at 37°C for 30 min in normal aCSF (as low-calcium aCSF above with 1 mM $MgCl_2$ and 2 mM $CaCl_2$) and thereafter maintained at room temperature (23–25°C) until required.

Electrophysiological recordings. Whole-cell patch-clamp recordings of calyces of Held were made under visual control using differential interference illumination in an upright microscope (BX50WI; Olympus, To-Tokyo, Japan). Calcium influx was evoked by applying depolarizing pulses in voltage-clamp mode. Patch pipettes with a resistance of 4.5–5.5 MΩ were used for recordings. The standard K^+ pipette solution contained the following (in mM): 120 K gluconate, 30 KCl, 20 HEPES, 4 MgATP, 4 Na ascorbate, and 0.3 NaGTP at pH 7.3 (adjusted with KOH). For a K^+-free pipette solution, K gluconate and KCl in the K^+ pipette solution were replaced with equimolar tetraethylammonium (TEA)-Cl. Alternatively, to rule out the possibility of organic cations inhibiting the K^+-independent form of Na/CaX (NCX), K^+ ions in the K^+ pipette solution were replaced with Li^+ ions (Blaustein, 1977). Recordings were made in calyces of Held using an EPC-9 amplifier (HEKA Elektronik, Lambrecht, Germany). During recordings, series resistances were compensated up to 85% with a 10 μs lag time. Recordings were terminated when the series resistance exceeded 30 MΩ. Experiments were performed at 35 ± 1°C. All chemicals were obtained from Sigma (St. Louis, MO), except 5(6)-carboxyeosin diacetate (CE) and fura-2FF from Fluka (Buchs, Switzerland) and fura-4F from Molecular Probes (Eugene, OR).

Cytosolic Ca^{2+} measurements. The procedures for cytosolic Ca^{2+} measurement in slices have been described previously in detail (Kim et al., 2003). Ca^{2+} concentrations were measured by fluorescence imaging. Cells were loaded with fura-4F or fura-2FF (pentapotassium salts; 50 μM each) via patch electrodes. For fluorescence excitation, we used a polychromatic light source (xenon lamp based; Polychrome-II; TILL Photonics, Gräfelfing, Germany), which was coupled to the epiillumination port of an upright microscope (BX50; Olympus) via a quartz light guide and a UV condenser. Imaging was performed using a 60× water immersion objective (numerical aperture, 0.9; LUMPlanFl; Olympus) and an air-cooled slow-scan CCD camera (SensiCam; PCO, Kelheim, Germany). The monochromator and the CCD camera were controlled by a personal computer, running a custom-made software programmed with MicroSoft Visual C++ (version 6.0).

The ratio ($R = F_{iso}/F_{380}$) of fluorescence at the isosbestic wavelength (360 nm; F_{iso}) to that at 380 nm (F_{380}) was converted to $[Ca^{2+}]_i$ according to the following equation:

$$[Ca^{2+}]_i = K_{eff} \cdot (R - R_{min})/(R_{max} - R). \quad (1)$$

Calibration parameters were determined by "in-cell" calibration as described by Lee et al. (2000). R_{min} values were measured using a Ca^{2+}-free pipette solution containing 10 mM BAPTA. R_{max} values were obtained from *in vitro* measurements, because calyces of Held did not endure internal dialysis with high $CaCl_2$ (10 mM). The values for the calibration ratio at intermediate $[Ca^{2+}]_i$ were measured using a pipette solution containing 5 mM BAPTA and 3.5 mM $CaCl_2$ ($[Ca^{2+}]_i \approx 540$ nM) for fura-4F and a pipette solution containing 80 mM DPTA and 10 mM $CaCl_2$ ($[Ca^{2+}]_i \approx 10$ μM) for fura-2FF. The effective dissociation constant of fura-2 (K_{eff}) was calculated by measuring the fluorescence ratio at these intermediate $[Ca^{2+}]_i$ and by rearranging Equation 1 for K_{eff}. The K_d values of fura-4F and fura-2FF were calculated as 0.79 and 3.1 μM, respectively, from $K_d = K_{eff} \cdot (\alpha + R_{min})/(\alpha + R_{max})$, where α is the isocoefficient (Zhou and Neher, 1993). To increase time resolution and minimize the photobleaching effect, we adopted a single-wavelength protocol (Helmchen et al., 1996; Lee et al., 2000) and pixels were binned by 8 × 8, which allowed exposure times of 5 ms. Images taken at 40 Hz with a single-wavelength excitation at 380 nm (F_{380}) were preceded and followed by images taken with excitation at isosbestic wavelengths (360 nm). F_{iso} (isosbestic fluorescence) values were linearly interpolated between points just before and after the period of excitation at 380 nm.

Calculation of total Ca^{2+} clearance rate. We measured the decay rate of free Ca^{2+} from the time derivative of the decay phase of a Ca^{2+} transient ($d[Ca^{2+}]_i/dt$). Because genuine Ca^{2+} clearance rate of a cell is represented by the clearance rate of total calcium ($d[Ca^{2+}]_T/dt$) rather than by decay rate of free calcium, $d[Ca^{2+}]_i/dt$ was converted to $d[Ca^{2+}]_T/dt$ using the following relationship:

$$d[Ca^{2+}]_T/dt = d[Ca^{2+}]_i/dt \cdot (\kappa_S + \kappa_B + 1) \quad (2)$$

where κ_S and κ_B represent the calcium binding ratios of the endogenous and exogenous buffers, respectively (Neher and Augustine, 1992; Kim et al., 2003).

When the decay phase of a Ca^{2+} transient is fitted with the following biexponential function:

$$[Ca^{2+}]_i(t) = A_0 + A_1 \cdot \exp(-\lambda_1 \cdot t) + A_2 \cdot \exp(-\lambda_2 \times t), \quad (3)$$

the Ca^{2+} decay rate at the peak of the Ca^{2+} transient can be represented by a time derivative of the biexponential function estimated at $t = 0$ as follows:

$$(-d[Ca^{2+}]_i/dt)_{t=0} = A_1 \cdot \lambda_1 + A_2 \cdot \lambda_2 \quad (4)$$

where A and λ represent amplitude and rate constant (inverse of time constant) of each component, respectively. In addition, according to Equation 2, the total Ca^{2+} clearance rate at the peak of a Ca^{2+} transient can be calculated by the following:

$$(-d[Ca^{2+}]_T/dt)_{t=0} = (A_1 \cdot \lambda_1 + A_2 \cdot \lambda_2) \cdot (\kappa_S + \kappa_B + 1) \quad (5)$$

Calculation of Ca^{2+} decay rate constant at the peak ($\lambda_{t=0}$). Although the decay phase of Ca^{2+} transients in this study were best fitted with the biexponential function, each (fast or slow) component of the biexponential fit does not necessarily reflect the activity of a single entity of Ca^{2+} clearance mechanism, because the Ca^{2+} clearance caused by each CCM was not constant but is nonlinearly dependent on the $[Ca^{2+}]_i$ excursion from resting level ($\Delta[Ca^{2+}]_i$) (see Figs. 1*D*, 2*Bb*, dotted lines). Thus, for statistical comparison of Ca^{2+} clearance measured from different cells and/or different experimental conditions, the decay rate at the peak was normalized by the peak $\Delta[Ca^{2+}]_i$ level ($\Delta[Ca^{2+}]_{peak}$), resulting in a Ca^{2+} decay rate constant at the peak ($\lambda_{t=0}$), which is defined as follows: $(-d[Ca^{2+}]_i/dt)_{t=0}/\Delta[Ca^{2+}]_{peak}$ (Kim et al., 2003). In the particular

case in which the Ca^{2+} decay is biexponential, $\lambda_{t=0}$ can be calculated by the following equation:

$$\lambda_{t=0} = (A_1 \cdot \lambda_1 + A_2 \cdot \lambda_2)/(A_1 + A_2) \quad (6)$$

Although the relationship between $d[Ca^{2+}]_i/dt$ and $\Delta[Ca^{2+}]_i$ is not linear over the entire range of $\Delta[Ca^{2+}]_i$, the relationship is almost linear when $\Delta[Ca^{2+}]_i$ is between 0.6 and 2.5 μM (see Figs. 1–4, plots of $d[Ca^{2+}]_T/dt$ vs $\Delta[Ca^{2+}]_i$). In this range of $\Delta[Ca^{2+}]_i$, $\lambda_{t=0}$ is constant, independent of $\Delta[Ca^{2+}]_i$, especially when peak $\Delta[Ca^{2+}]_i$ levels vary within a relatively narrow range. Thus, we adjusted the depolarizing pulse such that the peak $\Delta[Ca^{2+}]_i$ level of a Ca^{2+} transient fell between 2 and 2.5 μM, and we used $\lambda_{t=0}$ as a parameter to statistically compare the Ca^{2+} clearance rates.

Calculation of relative contribution of a clearance mechanism. The contribution of a clearance mechanism, Φ, to the entire Ca^{2+} clearance at a given $\Delta[Ca^{2+}]_i$ level has been described previously (Kim et al., 2003). From the time derivatives ($d[Ca^{2+}]_i/dt$) of the decay phases of two Ca^{2+} transients before and after treatment with an inhibitor of Φ, total Ca^{2+} clearance rate ($d[Ca^{2+}]_T/dt$) was calculated and plotted as a function of $\Delta[Ca^{2+}]_i$ (Eq. 2). The difference between the polynomial fit ($f_{control}$) to the $d[Ca^{2+}]_T/dt$ curve under control condition and that ($f_{inhibitor}$) in the presence of the inhibitor was regarded as the contribution made by Φ, and the relative contribution made by $\Phi(R_\Phi)$ to the entire Ca^{2+} clearance mechanism can be expressed as follows:

$$R_\Phi = (f_{control} - f_{inhibitor})/f_{control} \quad (7)$$

Data analysis. Data were analyzed using IgorPro (version 4.1; WaveMetrics, Lake Oswego, OR). Statistical data are expressed as mean ± SEM, and *n* indicates the number of cells studied. The significance of differences between Ca^{2+} decay rate constants was evaluated using paired or nonpaired Student's *t* test using a significance level of 0.05.

Results

We investigated Ca^{2+} clearance mechanisms at the calyx of Held (Fig. 1*A*) by analyzing the decay of Ca^{2+} transients obtained from fluorescent Ca^{2+} imaging. Calyces of Held were loaded via a patch pipette with an internal solution containing 50 μM fura-4F or fura-2FF, and Ca^{2+} transients were evoked by applying a short depolarizing pulse (from a holding potential of −80 or −70 mV to 0 mV; 50 ms in duration). The decay phases of the Ca^{2+} transients were well fitted by biexponential functions ($\chi^2 < 0.05$), and the fitting parameters in various experimental conditions are summarized in Table 1. The clearance is defined as a decay rate constant (τ^{-1}) in the case of a monoexponential decay. To obtain the parameter representing the Ca^{2+} clearance from biexponential Ca^{2+} decay rates, we adopted a weighted average of two decay rate constants ($\lambda_{t=0}$) (see Materials and Methods), which is mathematically the same as the decay rate at the peak divided by the amplitude of a biexponential Ca^{2+} transient $[(-d[Ca^{2+}]_i/dt)_{t=0}/\Delta[Ca^{2+}]_{peak}]$. Thus, we refer to $\lambda_{t=0}$ as a Ca^{2+} decay rate constant at the peak (see Materials and Methods). Because the relative amplitude of the fast component was >80% in this study, the value for $\lambda_{t=0}$ is quite close to τ_{fast}^{-1} (Fig. 1*C*).

Na^+/Ca^{2+} exchange is a major CCM at the calyx of Held

To investigate the contribution of Na/CaXs to Ca^{2+} clearance, we examined the effect of $[Na^+]_o$ reduction (replacement of the 125 mM NaCl in the bathing solution with equimolar LiCl) on the Ca^{2+} decay. The calyces were stimulated by a depolarization pulse (50 ms) to 0 mV in voltage-clamp mode. With the standard K^+ pipette solution (see Materials and Methods), $[Na^+]_o$ reduction significantly reduced the Ca^{2+} decay rate (Fig. 1*Ba*). Mean values for fast (τ_{fast}) and slow (τ_{slow}) time constants in control condition (Fig. 1*Ba*, black line) were 74.2 ± 4.1 and 975.4 ±

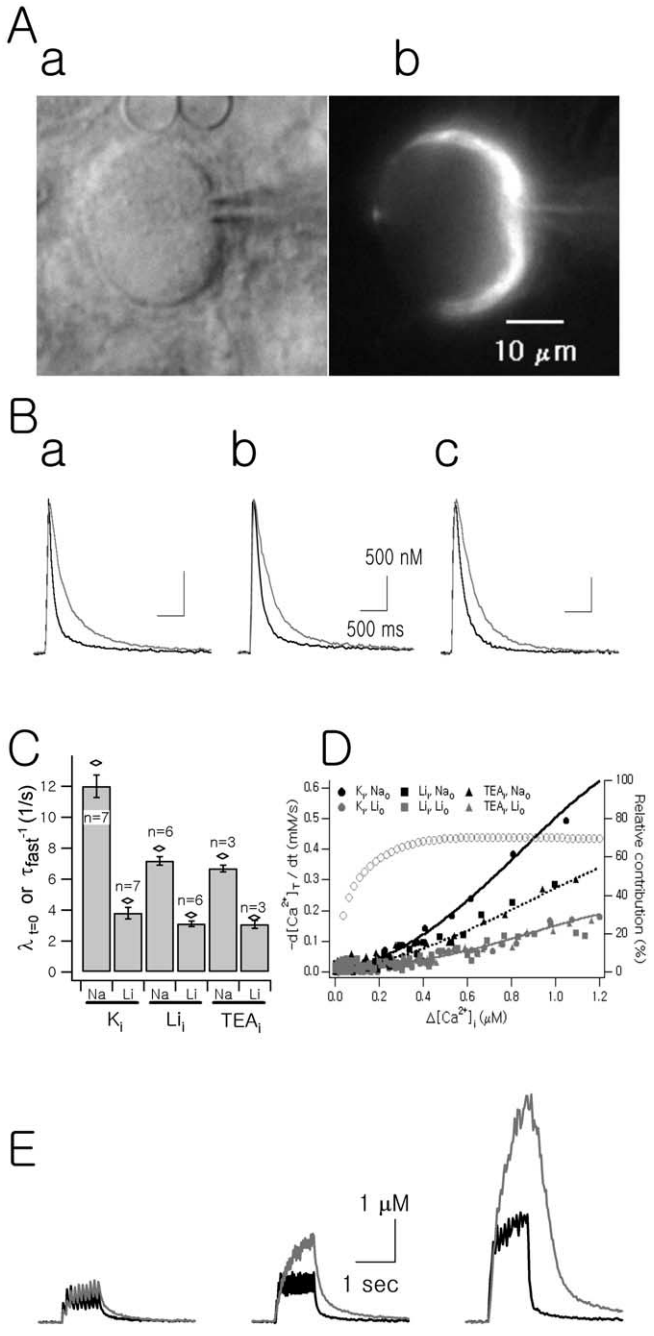

Figure 1. Contribution of Na^+/Ca^{2+} exchange to presynaptic Ca^{2+} clearance. ***A***, An image of the calyx of Held surrounding the postsynaptic MNTB neuron (***Aa***, DIC image; ***Ab***, Ca^{2+} fluorescence image). ***B***, Ca^{2+} transients evoked by a 50 ms depolarizing pulse from −70 to 0 mV at the calyx of Held recorded with a K^+ pipette (***Ba***), with a Li^+ pipette (***Bb***), and with a TEA^+ pipette (***Bc***). Two Ca^{2+} transients recorded at $[Na^+]_o$ of 145 mM (black line) and at $[Na^+]_o$ of 25 mM (gray line; Na^+ was replaced by Li^+) are superimposed in each panel. ***C***, Mean values for $\lambda_{t=0}$ (bar graph) and for τ_{fast} (diamonds) of Ca^{2+} transients. ***D***, Total Ca^{2+} clearance rate ($-d[Ca^{2+}]_T/dt$) calculated from the time derivatives of the decay phases of six Ca^{2+} transients shown in ***B*** (circles, K^+ pipette; squares, Li^+ pipette; triangles, TEA^+ pipette). Fifth-order polynomial fits are superimposed on the plots (continuous lines). Relative contributions of Na/CaX to total Ca^{2+} clearance were plotted as a function of $\Delta[Ca^{2+}]_i$ (open circles, right axis). ***E***, Representative Ca^{2+} records evoked by train pulses at various frequencies under normal $[Na^+]_o$ and 25 mM $[Na^+]_o$ conditions. Ca^{2+} transients were evoked by trains of 2 ms depolarization pulses at frequencies of 10 Hz (left), 20 Hz (middle), or 50 Hz (right) for 1 s. K^+-rich solution was used as a pipette solution. $\Delta[Ca^{2+}]_i$ induced by 10, 20, and 50 Hz train depolarization in normal aCSF were 0.84, 1.16, and 2.55 μM (black traces) and, after $[Na^+]_o$ reduction, were 0.98, 2.05, and 5.32 μM (gray traces), respectively.

108.7 ms ($n = 7$), respectively. After $[Na^+]_o$ reduction (Fig. 1*Ba*, gray line), the increase in the fast time constant (τ_{fast}) was more significant (218.7 ± 13.5 ms; $n = 7$; paired t test, $p < 0.01$) than the increase in the slow time constant (τ_{slow}; 1428.2 ± 236.0 ms; $n = 7$; paired t test, $p > 0.05$) (Table 1). The preferential deceleration (approximately threefold) of the fast decay phase under the low $[Na^+]_o$ condition suggests that Na/CaX is a Ca^{2+} clearance mechanism of high-capacity and low-affinity at the calyx of Held.

We next tested whether the Na/CaX activity depends on intracellular K^+. For this purpose, we recorded the Ca^{2+} transients using K^+-free pipette solutions. Figure 1, *Bb* and *Bc*, shows the representative Ca^{2+} transients recorded with Li^+ and TEA^+ pipette solutions, respectively. The Ca^{2+} transients in normal $[Na^+]_o$ (black line) and after the $Na^+{}_o$ replacement (gray line) were superimposed for each recording condition. In normal $[Na^+]_o$ condition, the decay rate constants ($\lambda_{t=0}$) of the Ca^{2+} transients recorded with Li^+ and TEA^+ pipettes were 7.18 ± 0.27 s^{-1} ($n = 6$) and 6.69 ± 0.22 s^{-1} ($n = 3$), respectively (Fig. 1*C*). These values are significantly lower than that with the K^+ pipette (12.01 ± 0.72 s^{-1}; $p < 0.01$) (Fig. 1*C*). The slower decay rate constant in the K^+-free internal condition suggests that NCKXs contribute to Ca^{2+} clearance at the calyx of Held. Under the K^+-free internal condition, $[Na^+]_o$ reduction further decreased the Ca^{2+} decay rate (Fig. 1*Bb*,*Bc*, gray traces). When the Na^+ gradient was reduced, the decay rate constants were reduced to 3.12 ± 0.17 s^{-1} in the Li^+ pipette condition and to 3.09 ± 0.25 s^{-1} in the TEA^+ pipette condition, which are similar to that in the K^+ pipette condition (3.80 ± 0.37 s^{-1}; $p > 0.05$) (Fig. 1*C*). These results show that Na/CaX activity still remained even in the absence of internal K^+, suggesting that both NCX and NCKX contribute to the calcium clearance at the calyx of Held.

To quantify the relative contributions of NCX and NCKX, the decrease in the Ca^{2+} decay rate constant ($\lambda_{t=0}$) caused by low $[Na^+]_o$ in the K^+ pipette condition was compared with those in the K^+-free pipette condition. The relative contributions of NCKX according to the equations $(\lambda_{t=0,K\_Na} - \lambda_{t=0,Li\_Na})/\lambda_{t=0,K\_Na}$ and $(\lambda_{t=0,K\_Na} - \lambda_{t=0,TEA\_Na})/\lambda_{t=0,K\_Na}$ were estimated to be ~41 and 45%, respectively (the first subscripts, K, Li, and TEA, represent major internal cations, and the second subscripts, Na and Li, represent major external cations). Similarly, the contributions of NCX according to $(\lambda_{t=0,Li\_Na} - \lambda_{t=0,K\_Li})/\lambda_{t=0,K\_Na}$ and $(\lambda_{t=0,TEA\_Na} - \lambda_{t=0,K\_Li})/\lambda_{t=0,K\_Na}$ were 28.2 and 24.0%, respectively. NCKX and NCX were responsible for ~42 and 26% of total Ca^{2+} clearance, respectively. The overall contribution of Na/CaXs, including both NCX and NCKX, was calculated using $(\lambda_{t=0,K\_Na} - \lambda_{t=0,K\_Li})/\lambda_{t=0,K\_Na}$ to be 68.6 ± 1.7%.

To estimate the relative contribution of Na/CaX to the entire Ca^{2+} clearance as a function of the $\Delta[Ca^{2+}]_i$ level, the total Ca^{2+} clearance rate ($-d[Ca^{2+}]_T/dt$) was calculated from the time derivative of the decay phase of a Ca^{2+} transient according to Equation 2, using a κ_S value of 40 (Helmchen et al., 1997) (Fig. 1*D*). From the polynomial fits to $-d[Ca^{2+}]_T/dt$ measured before (f_{K_Na}) (Fig. 1*D*, black solid line) and after (f_{K_Li}) (Fig. 1*D*, gray solid line) $[Na^+]_o$ reduction in the K^+ pipette condition, we calculated the relative contribution of Na/CaX according to the equation $(f_{K\_Na} - f_{K\_Li})/f_{K\_Na}$ (Fig. 1*D*, open circles, right axis). The relative contribution of Na/CaX increased as $\Delta[Ca^{2+}]_i$ increased to reach a maximum value (69%) at $\Delta[Ca^{2+}]_i > 400$ nM. We conclude that Na/CaX is the primary CCM in the calyx of Held in response to brief $\Delta[Ca^{2+}]_i$ elevations in the range of 1–2 μM. Our experiments under different internal ionic conditions suggest that Na/CaX is a major Ca^{2+} clearance mechanism, and that both NCX and NCKX contribute to Na/CaX in the calyx of Held.

Calyces of Held in young rats [postnatal day 8 (P8) to P10] can follow discharge rates up to 200 Hz (Borst et al., 1995), and the calyx of Held in adult mice receives and follows higher input frequencies of up to 600 Hz (Wu and Kelly, 1993). We examined the role of Na/CaX in Ca^{2+} clearance when Ca^{2+} transients were evoked by repetitive depolarization pulses (2 ms in duration) at frequencies of 10, 20, or 50 Hz for 1 s. The $\Delta[Ca^{2+}]_i$ during the 10 or 20 Hz stimulation underwent a fast rising phase and reached a plateau within 300 ms under control condition (Fig. 1*E*, black lines), but at 50 Hz stimulation, the fast rising phase was followed by a slower rising phase. Linear summation of Ca^{2+} transients predicts that the time required to reach the steady state is determined by the decay time constant of a single Ca^{2+} transient (Regehr et al., 1994; Helmchen et al., 1996). Consistently, after $[Na^+]_o$ reduction, the $\Delta[Ca^{2+}]_i$ level continued to build up throughout the train of pulses (1 s), and thus $\Delta[Ca^{2+}]_i$ at the end of the stimulation was greatly increased (Fig. 1*E*, gray lines). At a stimulation frequency of 50 Hz, the amplitudes of $\Delta[Ca^{2+}]_i$ before and after $[Na^+]_o$ reduction were 1.88 ± 0.37 and 4.95 ± 0.19 μM, respectively ($n = 3$) (Fig. 1*E*). These results indicate that Na/CaXs dampen presynaptic Ca^{2+} load very efficiently. Such efficient Ca^{2+} clearance seems to be essential for presynaptic

Table 1. Decay kinetics of Ca^{2+} transients measured using internal 50 μM Fura-4F at various experimental conditions

Conditions		n	τ_{fast} (ms)	τ_{slow} (ms)	$A_{slow}/A_{fast + slow}$ (%)
Na/CaX					
K_i	Control	7	74.2 ± 4.1	975.4 ± 108.7	11.7 ± 1.4
	Low Na^+		218.7 ± 13.5*	1428.2 ± 236.0	18.8 ± 3.1
Li_i	Control	6	125.8 ± 4.2	1552.1 ± 177.0	11.0 ± 1.5
	Low Na^+		274.4 ± 11.6*	1971.4 ± 197.4	17.4 ± 3.6
TEA_i	Control	3	134.2 ± 4.4	1036.4 ± 58.5	12.7 ± 0.2
	Low Na^+		287.9 ± 8.3*	1968.6 ± 311.5*	9.3 ± 2.1
SERCA inhibitors					
K_i	Control	5	77.6 ± 4.4	1230.3 ± 178.5	10.2 ± 1.0
	TG		81.1 ± 5.1	1270.7 ± 142.2	9.1 ± 0.6
	Control	3	72.3 ± 5.1	1100.7 ± 148.6	9.0 ± 1.2
	CPA		72.5 ± 4.9	1172.2 ± 129.3	10.7 ± 1.4
PMCA inhibitor					
K_i	Control	6	75.4 ± 4.4	1201.1 ± 140.4	10.1 ± 0.8
	CE		96.1 ± 4.3*	1592.4 ± 123.4*	13.2 ± 1.0
Mitochondria inhibitor					
K_i	Control	3	80.7 ± 12.6	1081.3 ± 237.3	10.2 ± 2.7
	CCCP		77.2 ± 7.6	1070.4 ± 107.5	11.1 ± 2.9
TEA_i	Control	3	131.5 ± 13.1	1179.0 ± 225.3	12.8 ± 5.6
	CCCP		204.0 ± 23.3*	1257.4 ± 230.0	16.1 ± 6.9
Ca^{2+} indicator dyes (50 μM)					
K_i	Fura-4F	24	75.8 ± 2.3	1113.8 ± 66.6	10.5 ± 0.6
	Fura-2FF	6	48.6 ± 2.0*	1278.6 ± 346.6	4.8 ± 0.4

Ca^{2+} transients were evoked by a 50 ms depolarization step at 35°C. Only Ca^{2+} transients with amplitudes that were within the range of 2–2.5 μM were included in the statistical analysis. The decay phase of a Ca^{2+} transient was fitted using a biexponential function. The parameters that provided a best fit under each condition are presented as mean ± SEM.

*Statistical significance compared with control value ($p < 0.05$).

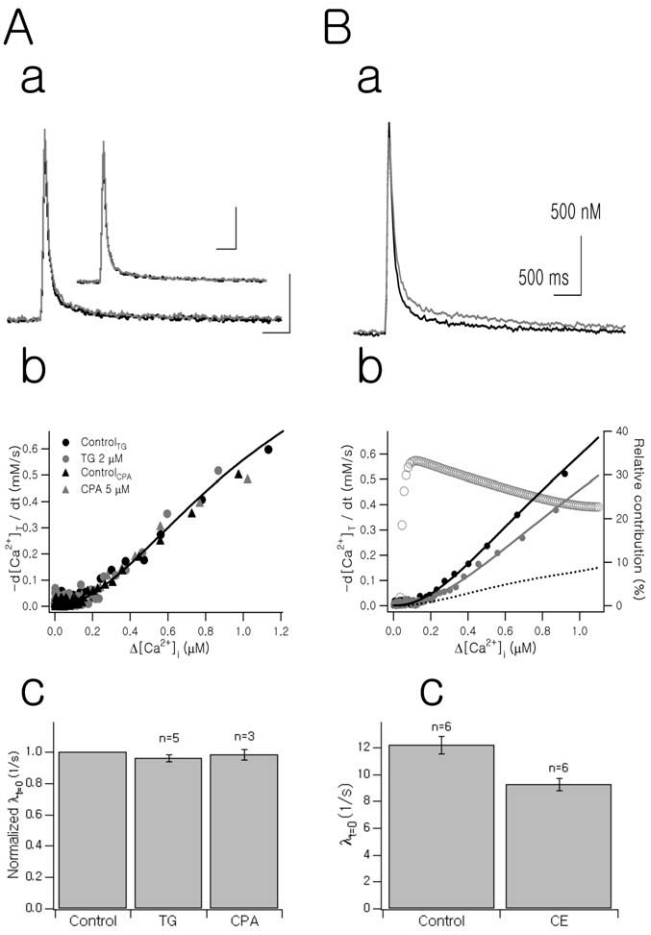

Figure 2. Effects of SERCA or PMCA pumps inhibitors on Ca^{2+} transients. ***Aa***, Representative Ca^{2+} transients recorded under the control condition (black line) and in the presence of 2 μM TG (gray line). Inset, Two Ca^{2+} transients recorded under the control condition (black line) and in the presence of 5 μM CPA (gray line). Calibration: 500 ms, 500 nM. ***Ab***, Total Ca^{2+} clearance rate ($-d[Ca^{2+}]_T/dt$) calculated from the decay phases of four Ca^{2+} transients shown in ***Aa***. Fifth-order polynomial fits were superimposed on the plots (continuous lines). ***Ac***, Mean values for $\lambda_{t=0}$ were normalized to those of the control condition and are depicted as a bar graph. ***Ba***, Ca^{2+} transients recorded under the control condition (black line) and in the presence of 40 μM CE (gray line), a PMCA pumps inhibitor, are superimposed. ***Bb***, $-d[Ca^{2+}]_T/dt$ were calculated from two Ca^{2+} transients, as shown in ***Ba***, and fitted with fifth-order polynomial functions. Differences between the two polynomial fits (dotted line) and the relative contribution of PMCA pumps to total Ca^{2+} clearance (gray open circles; right axis) are plotted. ***Bc***, Mean $\lambda_{t=0}$ values are the average of six cells.

axon terminals to transduce high-frequency spike input to synaptic release of neurotransmitter and to maintain presynaptic Ca^{2+} homeostasis.

Contribution of SERCA and PMCA pumps to presynaptic Ca^{2+} clearance

To investigate the contributions of SERCA and PMCA to Ca^{2+} clearance, we examined the effects of specific inhibitors of SERCA and PMCA on the Ca^{2+} decay rate measured with the K^+ pipette solution containing 50 μM fura-4F.

Inhibition of SERCA by the application of 2 μM thapsigargin (TG) to the bath had no effect on Ca^{2+} transients (Fig. 2*Aa*). The Ca^{2+} transients obtained before and after SERCA inhibition were superimposable. Another SERCA inhibitor, 5 μM cyclopiazonic acid (CPA), also had no effect (Fig. 2*Aa*, inset). The total Ca^{2+} clearance rate ($-d[Ca^{2+}]_T/dt$) as a function of $\Delta[Ca^{2+}]_i$ showed no difference before and after SERCA inhibition (Fig. 2*Ab*). These results suggest that SERCA contributes little to Ca^{2+} clearance, in agreement with previous work at the calyx of Held (Billups and Forsythe, 2002; Chuhma and Ohmori, 2002).

The contribution of the PMCA to Ca^{2+} clearance was assayed using 40 μM CE, a blocker of PMCA (Gatto and Milanick, 1993; Bassani et al., 1995). The Ca^{2+} decay was slightly slowed by CE (Fig. 2*Ba*). After PMCA inhibition, both the fast and slow time constants of Ca^{2+} decay were significantly increased ($n = 6$; paired t test; $p < 0.01$) (Table 1). Because CE can inhibit SERCA as well as PMCA (Fierro et al., 1998), 2 μM TG was preapplied to inhibit SERCA in some experiments, but results obtained with and without pretreatment of TG were similar. In contrast to Na/CaX, the relative contribution of PMCA was higher at lower $\Delta[Ca^{2+}]_i$ levels and decreased as $\Delta[Ca^{2+}]_i$ increased (Fig. 2*Bb*, gray open circles, right axis), which indicates that PCMA is a CCM of low capacity and high affinity. Figure 2*Bc* summarizes the effect of carboxyeosin on Ca^{2+} decay rate constants. The relative contribution of PMCA calculated according to the equation $(\lambda_{t=0,\text{control}} - \lambda_{t=0,\text{CE}})/\lambda_{t=0,\text{control}}$ was 23.8 ± 1.7% at $\Delta[Ca^{2+}]_i$ of 1 μM.

Role of mitochondria in presynaptic Ca^{2+} clearance

The contribution of mitochondrial Ca^{2+} uptake to presynaptic CCM was investigated using the protonophore carbonyl cyanide *m*-chlorophenylhydrazone (CCCP), which dissipates mitochondrial membrane potential and inhibits mitochondrial Ca^{2+} uptake. The application of CCCP had no effect on the resting Ca^{2+} concentration (100 ~ 150 nM). In the K^+ pipette condition, the bath application of 2 μM CCCP had no effect on Ca^{2+} transients (Fig. 3*Aa*). However, when NCKX was inhibited by using a TEA^+ pipette solution, CCCP significantly slowed the Ca^{2+} decay rate (Fig. 3*Ab*). Plots of $-d[Ca^{2+}]_T/dt$ as a function of $\Delta[Ca^{2+}]_i$ before and after CCCP application are superimposed in Figure 3*B*, and *C* summarizes the effect of CCCP on the Ca^{2+} decay rate constants with K^+ and TEA^+ pipette conditions.

We further tested whether the mitochondrial contribution to the Ca^{2+} clearance occurred when Na/CaX was inhibited. Using the K^+ pipette, Ca^{2+} decay was slowed by $[Na^+]_o$ reduction (Fig. 3*D*; black line, normal aCSF; gray line, low Na^+ aCSF). The addition of 2 μM CCCP to the low $[Na^+]_o$ bath solution led to an additional slowing of Ca^{2+} decay (Fig. 3*D*, gray dotted line). This result contrasted with the finding that CCCP had no effect on the Ca^{2+} decay rate measured with a K^+ pipette in normal aCSF (Fig. 3*Aa*). When we reintroduced external Na^+ in the presence of CCCP, the Ca^{2+} transient was completely restored to the control condition level (Fig. 3*D*; black line, normal aCSF; black dotted line, normal aCSF plus 2 μM CCCP), indicating that mitochondria do not contribute to Ca^{2+} clearance when Na/CaX is fully functional. Consistently, $-d[Ca^{2+}]_T/dt$ plots calculated from control (normal aCSF) and recovery (normal aCSF plus 2 μM CCCP) data overlapped almost completely (Fig. 3*E*). The mean values for $\lambda_{t=0}$ in each condition are compared in Figure 2*F*. Whereas $\lambda_{t=0}$ was significantly reduced by CCCP when Na/CaX was inhibited ($p < 0.01$) (Fig. 3*F*), $\lambda_{t=0}$ measured when $[Na^+]_o$ was reintroduced did not differ from that determined under the control condition despite the continued presence of CCCP ($p = 0.85$). These results imply that Na/CaX clears Ca^{2+} loads more readily than mitochondria, and that mitochondria, which compete for incoming Ca^{2+} with Na/CaX, take part in Ca^{2+} clearance only when Na/CaX is inhibited. In addition, the contribution of Na/CaX to Ca^{2+} clearance may be higher than our estimate (68%), because the inhibition of Na/CaX could be partially compensated by mitochondria under low $[Na^+]_o$ condition.

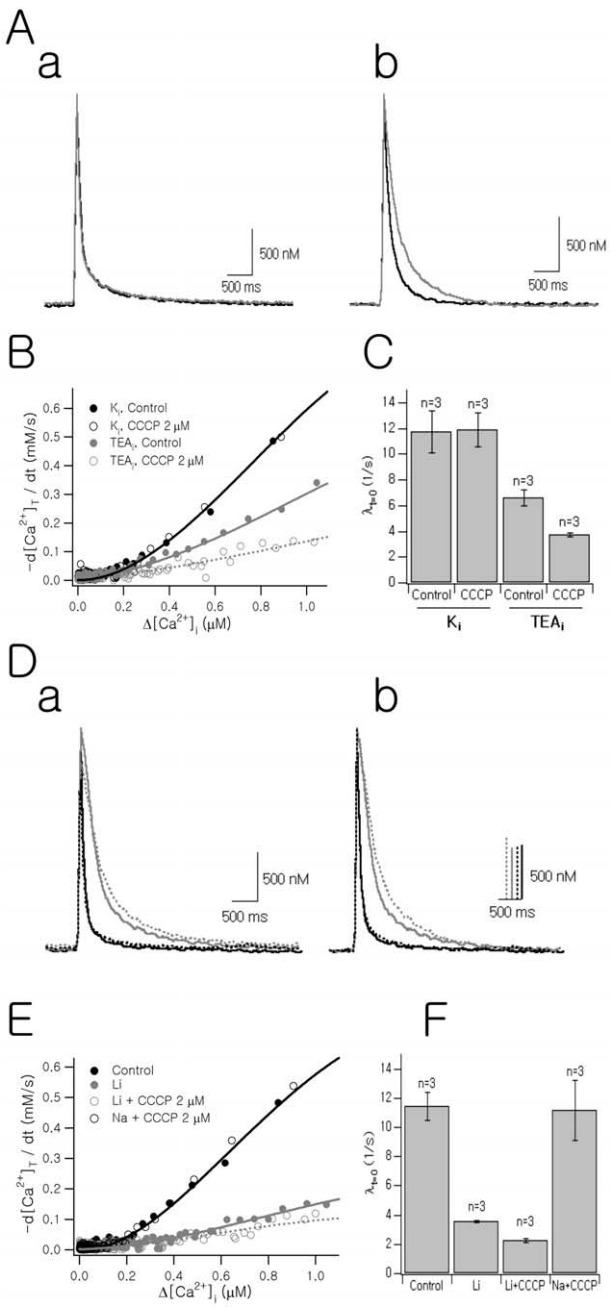

Figure 3. Interaction between Na^+/Ca^{2+} exchanger and mitochondrial Ca^{2+} uptake. ***Aa***, Two Ca^{2+} transients recorded with a K^+ pipette solution under the control condition (black line) and in the presence of 2 μM CCCP (gray line) were superimposed. ***Ab***, Ca^{2+} transients recorded with a TEA^+ pipette solution (black line: control condition; gray line: CCCP). ***B***, $-d[Ca^{2+}]_T/dt$ were calculated from four Ca^{2+} transients as shown in ***A***. ***C***, Mean values for $\lambda_{t=0}$ of Ca^{2+} transients under the conditions indicated below the abscissa. Mean values of $\lambda_{t=0}$ measured before and after the application of 2 μM CCCP were 11.73 ± 1.63 and 11.87 ± 1.30 s^{-1} for the K^+ pipette condition (paired *t* test; $n = 3$; $p = 0.73$) and 6.57 ± 0.65 and 3.76 ± 0.17 s^{-1} for TEA^+ pipette condition (paired *t* test; $n = 3$; $p < 0.05$). ***D***, Effects of CCCP on Ca^{2+} clearance when Na/CaX was inhibited. ***Da***, Four Ca^{2+} transients recorded in the same cell were superimposed. Each Ca^{2+} transient was evoked by a 50 ms depolarizing pulse using a K^+ pipette solution. $[Na^+]_o$ reduction (replaced by 125 mM Li^+) significantly slowed Ca^{2+} decay (gray line) compared with the control condition (black line). The bath application of 2 μM CCCP further reduced the Ca^{2+} decay rate (gray dotted line) in the low $[Na^+]_o$ solution. When $[Na^+]_o$ was reintroduced, the Ca^{2+} decay rate returned to the control condition, although mitochondrial Ca^{2+} uptake was still inhibited by CCCP (black dotted line). ***Db***, Four Ca^{2+} transients shown in ***Da*** were scaled to the same maximum value and superimposed to directly compare the decay phases. ***E***, $-d[Ca^{2+}]_T/dt$ values were calculated from the Ca^{2+} transients shown in ***D***. ***F***, Mean $\lambda_{t=0}$ values of Ca^{2+} transients are the average of three cells.

Dependence of mitochondrial Ca^{2+} clearance on $\Delta[Ca^{2+}]_i$

Studies of mitochondrial Ca^{2+} uptake suggest that mitochondrial Ca^{2+} uptake requires a high local Ca^{2+} concentration in the micromolar range because of the low affinity of mitochondria for Ca^{2+} (Brini, 2003). Thus, we examined the mitochondrial contribution to Ca^{2+} clearance at higher $\Delta[Ca^{2+}]_i$ levels. To induce various peak $\Delta[Ca^{2+}]_i$ of up to 6 μM, we increased $[Ca^{2+}]_o$ to 5 mM, and applied a single-step pulse (50 ms in duration) of various depolarization levels. To avoid saturation of Ca^{2+} indicator dye, 50 μM fura-2FF ($K_d \approx 3.1$ μM) was used instead of fura-4F. Ca^{2+} decay rates measured using fura-2FF were more rapid than those measured with the same concentration of fura-4F, reflecting its lower affinity for Ca^{2+} (Table 1). When peak $\Delta[Ca^{2+}]_i$ was <2.5 μM, CCCP had no noticeable effect on Ca^{2+} transients (Fig. 4*A*, left traces), which is consistent with the results in Figure 3*A*. However, when peak $\Delta[Ca^{2+}]_i$ was higher than 3 μM, CCCP slowed Ca^{2+} decay, and this effect of CCCP became more obvious as peak $\Delta[Ca^{2+}]_i$ was further increased (Fig. 4*A*, middle and right).

We analyzed 11 pairs of Ca^{2+} transients obtained from five different calyces. The relative contribution of mitochondria (R_{mito}) in each pair of Ca^{2+} transients (before and after the CCCP treatment) was calculated according to the equation $(\lambda_{t=0,control} - \lambda_{t=0,CCCP})/\lambda_{t=0,control}$, and plotted as a function of $\Delta[Ca^{2+}]_i$ (Fig. 4*B*, triangles). The mean value for R_{mito} in the range of $\Delta[Ca^{2+}]_i > 2.5$ μM (filled triangles) was significantly higher than that in the lower range (Fig. 4*B*, open triangles) ($p < 0.01$). These results indicate that mitochondria begin to take part in Ca^{2+} clearance when $\Delta[Ca^{2+}]_i$ is >2.5 μM.

For the same set of Ca^{2+} transients, we estimated total Ca^{2+} clearance rate at the peak $[(-d[Ca^{2+}]_T/dt)_{t=0}]$ according to Equation 5. Values for $(-d[Ca^{2+}]_T/dt)_{t=0}$ before (black circles) and after (gray circles) CCCP treatment are plotted as a function of peak $\Delta[Ca^{2+}]_i$ in Figure 4*C*. In addition, the data of $-d[Ca^{2+}]_T/dt$ obtained with fura-4F in lower $\Delta[Ca^{2+}]_i$ range (<1 μM) were superimposed (open circles). The composite graph of $-d[Ca^{2+}]_T/dt$ provides the dependence of $-d[Ca^{2+}]_T/dt$ on $\Delta[Ca^{2+}]_i$ over a wider range than the similar graph in Figure 3*B*. Although no effect of CCCP was observed at $\Delta[Ca^{2+}]_i < 2$ μM, CCCP downward-shifted the $-d[Ca^{2+}]_T/dt$ curve in the higher range of $\Delta[Ca^{2+}]_i$ (Fig. 4*C*, gray circles). In contrast, the $-d[Ca^{2+}]_T/dt$ values in the presence of thapsigargin (2 μM, crosses) were not different from the control condition, indicating that the SERCA did not contribute to Ca^{2+} clearance over the entire $\Delta[Ca^{2+}]_i$ range. It was also noted that the $-d[Ca^{2+}]_T/dt$ curve in the presence of CCCP showed saturation in the high $\Delta[Ca^{2+}]_i$ range. Considering that Na/CaX is the major CCM in such high $\Delta[Ca^{2+}]_i$ range, the $-d[Ca^{2+}]_T/dt$ curve might represent the saturation of Na/CaX activity (Fig. 4*C*, gray curve). In the absence of CCCP, the $-d[Ca^{2+}]_T/dt$ curve became more linear, indicating that the saturation of Na/CaX activity is partially compensated by the activation of mitochondrial Ca^{2+} uptake at $\Delta[Ca^{2+}]_i$ levels >2.5 μM.

Mitochondrial Ca^{2+} clearance and intracellular buffer concentration

We investigated the mechanisms whereby the inhibition or saturation of Na/CaX can render mitochondrial Ca^{2+} uptake active. We hypothesized that the inhibition or the saturation of Na/CaX allows mitochondria to be exposed to high cytosolic $[Ca^{2+}]$ for a longer duration. To test whether a longer exposure to high $[Ca^{2+}]_i$ is necessary for mitochondrial Ca^{2+} uptake in the calyx of Held, we slowed the Ca^{2+} decay rate by increasing the [fura-2FF] in the pipette solution instead of inhibiting Na/CaX, and

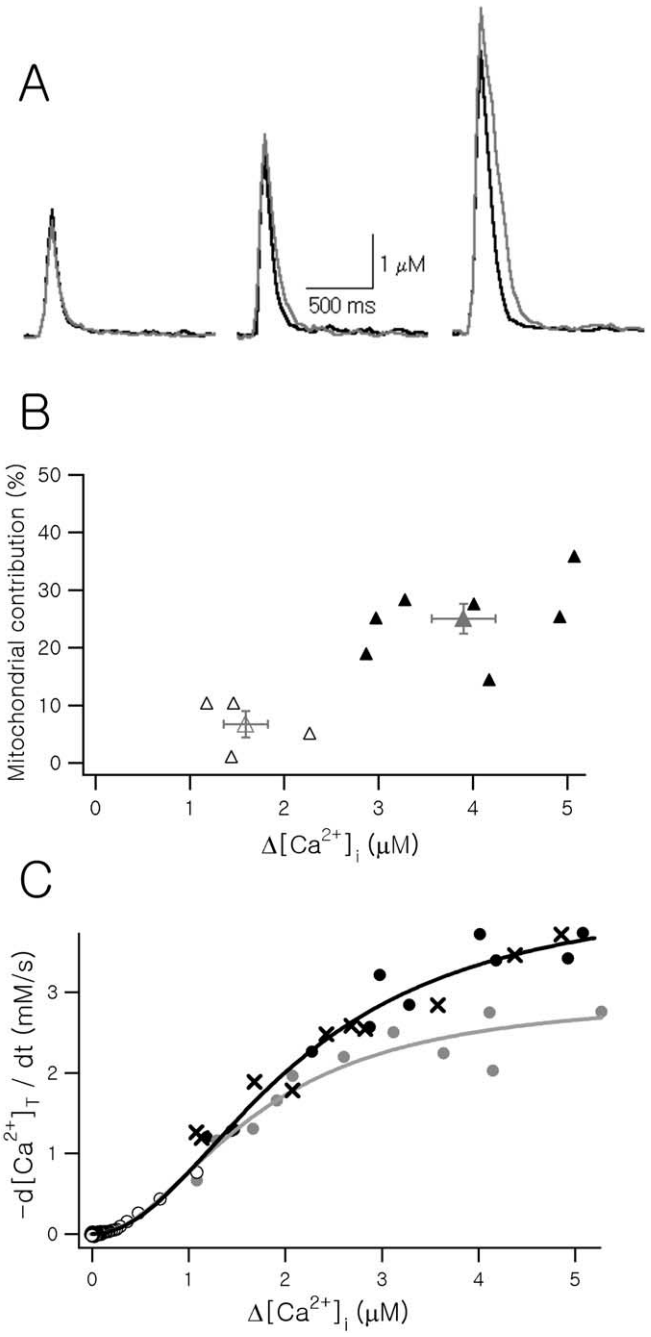

Figure 4. Effects of CCCP on Ca^{2+} clearance at various levels of $\Delta[Ca^{2+}]$. ***A***, Each pair of Ca^{2+} transients recorded with the K^+ pipette solution containing 50 μM fura-2FF in the control condition (black line) and in the presence of 2 μM CCCP (gray line) are superimposed. Three sets of Ca^{2+} transients were evoked by different levels of depolarization with a fixed 50 ms duration (left, −10 mV; middle, 0 mV; right, +10 mV). ***B***, Ca^{2+} decay rate constants ($\lambda_{t=0}$) for the CCCP condition were normalized to control values (open triangles, left ordinate). The relative contributions of mitochondria (R_{mito}) were calculated and plotted as a function of $\Delta[Ca^{2+}]_i$ (filled triangles). R_{mito} values whose $\Delta[Ca^{2+}]_i$ are below and those >2.5 μM were pooled, and mean values for two groups were superimposed (gray triangles). ***C***, $-d[Ca^{2+}]_T/dt$ values under the control (black circles) and under the CCCP condition (gray circles) as a function of $\Delta[Ca^{2+}]_i$. The values of $-d[Ca^{2+}]_T/dt$ were estimated from Ca^{2+} transients measured with fura-2FF in five different terminals (closed circles and crosses) and from those measured with fura-4F in four different terminals (open circles). The values in each set (set of control conditions or set of CCCP conditions) were pooled, and fitted using Hill's equation, $V_{max}/(1 + (K_{1/2}/[Ca^{2+}])^{HN})$, with the following parameters: $V_{max} = 4.30$ mM/s, $HN = 2$, and $K_{1/2} = 2.14$ μM for the control condition (black line); $V_{max} = 2.96$ mM/s, $HN = 2$, and $K_{1/2} = 1.7$ μM for the CCCP condition (gray line). The $-d[Ca^{2+}]_T/dt$ values determined in the presence of 2 μM thapsigargin were similar to those determined under the control condition (crosses).

examined the effect of CCCP on Ca^{2+} transients. Moreover, to avoid the saturation of Na/CaX, the peak $\Delta[Ca^{2+}]_i$ was adjusted to 2~2.5 μM by varying the membrane potential during the 50 ms depolarizations. At 50 μM fura-2FF (Fig. 5*Aa*), CCCP had little effect on Ca^{2+} transients. However, at higher $[\text{fura-2FF}]_i$ levels (Fig. 5*Ab*, 200 μM; *Ac*, 400 μM), the effects of CCCP on Ca^{2+} transients became evident. We obtained similar results when mitochondrial Ca^{2+} uptake was inhibited by 10 μM tetraphenylphosphonium (TPP^+), which has no effect on ATP production. Because the inhibition of the Ca^{2+} decay rate caused by CCCP was not statistically different from that caused by TPP^+, two data sets were pooled for statistical analysis. The mitochondrial contribution to the Ca^{2+} clearance at various concentrations of fura-2FF is summarized as a bar graph in Figure 5*B*, which shows that the effects of CCCP or TPP^+ increased as the fura-2FF concentration increased. The relative contribution of mitochondria to total Ca^{2+} clearance measured with 50, 200, and 400 μM fura-2FF were 8.4 ± 1.9, 24.1 ± 4.9, and 31.1 ± 5.3%, respectively. These results suggest that the slowed Ca^{2+} decay is a direct cause of mitochondrial Ca^{2+} uptake when Na/CaX is inhibited.

Discussion

Ca^{2+} signaling in axon terminals plays a crucial role in synaptic function. The Ca^{2+} clearance rate in axon terminals not only determines the duration and amplitude of a Ca^{2+} transient but also affects short-term plasticity by a mechanism involving residual calcium. In the present study, we quantified the contribution made by each putative CCM at the calyx of Held and demonstrate the role of NCKX in presynaptic Ca^{2+} clearance. In addition, we found that (1) Na/CaX, comprised of NCKX and NCX, is a major CCM in the calyx of Held; (2) PMCA is responsible for 23% of the Ca^{2+} clearance when $\Delta[Ca^{2+}]_i$ is <1 μM; and (3) mitochondria contribute to Ca^{2+} clearance only when Na/CaX is inhibited or when the Ca^{2+} load is high enough to saturate Na/CaX capacity.

Role of Na/CaX in the calyx of Held

Although calyces of Held are extremely large presynaptic terminals, their thin cuplike structure constitutes a high surface-to-volume ratio (Sätzler et al., 2002). In neuronal compartments with a high surface-to-volume ratio, CCMs in the plasma membrane may clear cytosolic Ca^{2+} more efficiently than other CCMs that sequestrate Ca^{2+} into intracellular organelles. Various axon terminals effectively clear Ca^{2+} using plasma membrane CCMs such as Na/CaX and PMCA (Gill et al., 1981; Sanchez-Armass and Blaustein, 1987; Reuter et al., 1995; Morgans et al., 1998; Zenisek et al., 2000; Chuhma and Ohmori, 2002; Lee et al., 2002). Our results indicate that Na/CaX is a primary CCM at the calyx of Held. Moreover, mitochondria play a supplementary role when Na/CaX is inhibited or its activity is saturated (Fig. 4). This interaction between Na/CaX and mitochondria is similar to that between PMCA and mitochondria in the presynaptic terminals of retinal bipolar neurons, in which PMCAs are the primary CCM and mitochondrial Ca^{2+} uptake is observed only when PMCAs are inhibited (Zenisek et al., 2000).

The calyx of Held synapse plays a pivotal role in sound localization, especially for high-frequency sounds (Oertel, 1999; von Gersdorff and Borst, 2002). Adult calyces of Held have been known to receive and follow APs of high frequency up to 600 Hz (Taschenberger and von Gersdorff, 2000). It is thought that, for accurate sound localization, calyces of Held relay high-frequency inputs to postsynaptic MNTB neurons with high fidelity. In order for a calyx of Held to synchronize repetitive electrical events with

transmitter release, presynaptic Ca^{2+} transients triggered by APs should be cleared immediately during an interspike interval so that the subsequent AP triggers a discrete Ca^{2+} transient. Na/CaX, which has a higher capacity for Ca^{2+} extrusion than other CCMs, seems to meet these requirements. Our results in Figure 1*E* show what happens to presynaptic $\Delta[Ca^{2+}]_i$ in the absence of Na/CaX when high-frequency APs invade the calyx of Held. When we stimulated the calyx of Held with trains of 2 ms depolarizing pulses at 10, 20, or 50 Hz, $\Delta[Ca^{2+}]_i$ reached a steady state in the range of 0.5~2 μM within 300 ms in the control condition, but the inhibition of Na/CaX caused a continued buildup of $[Ca^{2+}]_i$, which lasted for the stimulation duration (1 s).

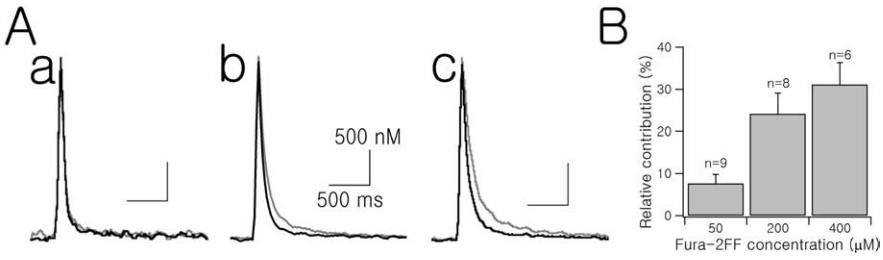

Figure 5. Effects of exogenous buffer on mitochondrial Ca^{2+} uptake. ***Aa–Ac***, A pair of Ca^{2+} transients recorded at various [fura-2FF] in the control condition (black line) and in the presence of 2 μM CCCP (gray line) were superimposed. The [fura-2FF] in ***Aa***, ***Ab***, and ***Ac*** were 50, 200, and 400 μM, respectively. ***B***, The relative contribution made by mitochondria measured at [fura-2FF] of 50, 200, or 400 μM are summarized as a bar graph.

The range of spatially averaged Ca^{2+} signals observed in this study (0.5–6 μM) contrasts with the local $[Ca^{2+}]_i$ reached transiently at the sites of vesicle fusion during a presynaptic AP, which has been estimated at 10–25 μM for the calyx of Held (Bollmann et al., 2000; Schneggenburger and Neher, 2000). Thus, Na/CaX dampens the buildup of residual Ca^{2+}, but the termination of the local Ca^{2+} signal for transmitter release is probably achieved by cytosolic Ca^{2+} diffusion away from presynaptic active zones, after presynaptic Ca^{2+} channels close.

One would expect that presynaptic Na^+ influx during prolonged high-frequency trains of APs might dissipate transmembrane Na^+ gradient, which in turn would compromise the Na/CaX activity. Recently, it was reported that voltage-gated Na^+ channels are almost absent from the calyceal terminal and highly concentrated in the unmyelinated axonal heminode (Leao et al., 2005). The exclusion of Na^+ channels from the calyx might help to avoid a local build-up of $[Na^+]_i$ in the presynaptic terminal (but see Engel and Jonas, 2005).

Role of mitochondria in the calyx of Held

The present study shows that, at the calyx of Held, Na/CaX is the main CCM after brief bursts of presynaptic APs, which result in $\Delta[Ca^{2+}]_i \leq 2.5$ μM. However, mitochondria are expected to contribute to Ca^{2+} clearance when the function of Na/CaX is compromised or saturated.

The role of mitochondria in Ca^{2+} clearance observed here is somewhat different from that presented in a previous study, which used the same preparation (Billups and Forsythe, 2002). These authors reported that the inhibition of mitochondrial Ca^{2+} sequestration significantly slowed Ca^{2+} decay when $[Na^+]_o$ was not lowered. However, the experimental conditions used in the present study differ from those of Billups and Forsythe (2002) in several respects. First, these authors used a Cs^+ pipette solution containing a relatively high $[Na^+]_i$ (34 mM), whereas a K^+ pipette solution with a low $[Na^+]_i$ (4 mM) was used in the present study. Assuming a single Eyring barrier and a 3 Na^+:1 Ca^{2+} stoichiometry for NCX, Ca^{2+} efflux via NCX (J_{NCX}) is heavily dependent on the transmembrane Na^+ gradient as the following thermodynamic relationship suggests:

$$J_{NCX} \propto [Ca^{2+}]_i [Na]_o^3 \exp(-E_m F/2RT) - [Ca^{2+}]_o [Na]_i^3 \exp(E_m F/2RT),$$

where E_m, F, R, and T are membrane potential, the Faraday constant, the gas constant, and temperature, respectively. When $[Ca^{2+}]_i = 2$ μM and $E_m = -70$ mV, J_{NCX} is lower at $[Na^+]_i = 34$ mM than when $[Na^+]_i = 4$ mM by a factor of 6.65. In addition, we measured the outward current (reverse mode) of NCKX2 (I_{NCKX}) heterologously expressed in HEK293 cells and found that Cs^+ only partially substitutes for K^+ (M.-H. Kim, W.-K. Ho, and S.-H. Lee, unpublished observation), and thus we used K^+ pipettes instead of Cs^+ to observe Ca^{2+} transients under more physiological conditions. As our data suggest, the mitochondrial contribution could have been exaggerated under the high $[Na^+]_i$ and K^+-free condition, which is unfavorable for the function of Na/CaX. Second, in the study by Billups and Forsythe (2002), $\Delta[Ca^{2+}]_i$ induced by repetitive depolarization pulses at frequencies of 100 Hz for 40 ms was ~8 μM. Under this condition, mitochondria could contribute to Ca^{2+} clearance, because Na/CaX activity might be saturated. Third, Billups and Forsythe (2002) used a higher concentration of intracellular Ca^{2+} buffer (i.e., 200 μM fura-2FF plus 200 μM EGTA in the pipette solution). Because the Ca^{2+} decay rate is inversely proportional to the calcium binding ratio, a higher concentration of exogenous Ca^{2+} buffer would lead to an increase in the mitochondrial contribution to Ca^{2+} clearance, as shown in Figure 5. Borst et al. (1995) reported that the EPSC amplitudes evoked by the stimulation of axon fibers were unchanged when presynaptic terminals were perfused with 50 μM BAPTA (or 200 μM EGTA). However, Helmchen et al. (1997) suggested that most endogenous buffer in the calyx of Held might be immobile. In the present study, when the $\Delta[Ca^{2+}]_i$ of a Ca^{2+} transient triggered by a single AP was 500 nM, our exogenous Ca^{2+} buffer condition (50 μM fura-4F) is in between those of these two studies in terms of the calcium binding ratio, κ_B (41.3 for 50 μM BAPTA; 32.8 for 50 μM fura-4F). In contrast, 200 μM fura-2FF plus 200 μM EGTA, the buffer condition used by Billups and Forsythe (2002), is higher ($\kappa_B \approx 102$) than known physiological buffer conditions ($\kappa_S = 40$) (Helmchen et al., 1997). Nevertheless, a recent immunohistochemical study revealed that the mobile Ca^{2+} buffers calretinin and parvalbumin are present in the presynaptic terminals of the MNTB. In addition, the expression of calretinin is not homogenous, and the proportion of calretinin-positive calyces increases during postnatal development (Felmy and Schneggenburger, 2004). In view of the fact that higher Ca^{2+} buffers favor mitochondrial Ca^{2+} clearance, it is possible that mitochondria play a more important role for Ca^{2+} clearance with ongoing developmental maturation of calyces of Held.

Physiological implications

Recent studies suggest that CCMs might be involved in posttetanic potentiation (PTP) by a mechanism of residual calcium. At the crayfish neuromuscular junction, posttetanic slow Ca^{2+} release from mitochondria subsequent to Ca^{2+} uptake during tetanic stimulation was proposed as an underlying mechanism for

residual calcium (Tang and Zucker, 1997). Because posttetanic Ca^{2+} release is preceded by mitochondrial Ca^{2+} uptake during tetanic stimulation, the conditions required for mitochondrial Ca^{2+} uptake are of particular interest in terms of understanding presynaptic residual calcium and the associated short-term synaptic plasticity induced by high-frequency activity. In addition, an involvement of the Na/CaX in the residual calcium has also been suggested, because PTP and presynaptic Ca^{2+} accumulation at the crayfish neuromuscular junction are promoted by the reverse-mode Na/CaX (Zhong et al., 2001). Functional and immunocytochemical evidence support the existence of Na/CaX in presynaptic terminals in mammalian central synapses (Reuter et al., 1995; Regehr, 1997). The role of Na/CaX in the mammalian synapses is further supported by a study that showed that paired-pulse facilitation and PTP are enhanced in the mice lacking NCX2 (Jeon et al., 2003). We showed that the relative contributions of Na/CaX and of mitochondria to Ca^{2+} clearance are not static, but interact dynamically depending on $\Delta[Ca^{2+}]_i$ level. These results suggest that high-frequency activity, which allows mitochondria to take up cytosolic Ca^{2+}, could cause short-term plastic changes at the calyx of Held synapse. Indeed, PTP of transmitter release has been observed recently at the calyx of Held (Habets and Borst, 2005; Korogod et al., 2005).

References

Bassani RA, Bassani JWM, Bers DM (1995) Relaxation in ferret ventricular myocytes: role of the sarcolemmal Ca ATPase. Pflügers Arch 430:573–578.

Billups B, Forsythe ID (2002) Presynaptic mitochondrial calcium sequestration influences transmission at mammalian central synapses. J Neurosci 22:5840–5847.

Blaustein MP (1977) Effects of internal and external cations and ATP on sodium-calcium exchange and calcium-calcium exchange in squid axons. Biophys J 20:79–111.

Bollmann JH, Sakmann B, Borst JGG (2000) Calcium sensitivity of glutamate release in a calyx-type terminal. Science 289:953–957.

Borst JG, Helmchen F, Sakmann B (1995) Pre- and postsynaptic whole-cell recordings in the medial nucleus of the trapezoid body of the rat. J Physiol (Lond) 489:825–840.

Brini M (2003) Ca^{2+} signalling in mitochondria: mechanism and role in physiology and pathology. Cell Calcium 34:399–405.

Chuhma N, Ohmori H (2002) Role of Ca^{2+} in the synchronization of transmitter release at calyceal synapses in the auditory system of rat. J Neurophysiol 87:222–228.

Engel D, Jonas P (2005) Presynaptic action potential amplification by voltage-gated Na^+ channels in hippocampal mossy fiber boutons. Neuron 45:405–417.

Felmy F, Schneggenburger R (2004) Developmental expression of the Ca^{2+}-binding proteins calretinin and parvalbumin at the calyx of Held of rats and mice. Eur J Neurosci 20:1473–1482.

Fierro L, DiPolo R, Llano I (1998) Intracellular calcium clearance in Purkinje cell somata from rat cerebellar slices. J Physiol (Lond) 510:499–512.

Gatto C, Milanick MA (1993) Inhibition of the red blood cell calcium pump by eosin and other fluorescein analogues. Am J Physiol 264:C1577–C1586.

Gill DL, Grollman EF, Kohn LD (1981) Calcium transport mechanisms in membrane vesicles from guinea pig brain synaptosomes. J Biol Chem 256:184–192.

Habets RL, Borst JG (2005) Post-tetanic potentiation in the calyx of Held synapse. J Physiol (Lond) 564:173–187.

Helmchen F, Imoto K, Sakmann B (1996) Ca^{2+} buffering and action potential-evoked Ca^{2+} signaling in dendrites of pyramidal neurons. Biophys J 70:1069–1081.

Helmchen F, Borst JGG, Sakmann B (1997) Calcium dynamics associated with a single action potential in a CNS presynaptic terminal. Biophys J 72:1458–1471.

Jeon DJ, Yang YM, Jeong MJ, Philipson KD, Rhim H, Shin HS (2003) Enhanced learning and memory in mice lacking Na^+/Ca^{2+} exchanger 2. Neuron 38:965–976.

Kim MH, Lee S, Park KH, Ho WK, Lee SH (2003) Distribution of K^+-dependent Na^+/Ca^{2+} exchangers in the rat supraoptic magnocellular neuron is polarized to axon terminals. J Neurosci 23:11673–11680.

Korogod N, Lou X, Schneggenburger R (2005) Presynaptic Ca^{2+}-requirements and developmental regulation of posttetanic potentiation at the calyx of Held. J Neurosci 25:5127–5137.

Leao RM, Kushimerick C, Pinaud R, Renden R, Li GL, Taschenberger H, Spirou G, Levinson SR, von Gersdorff H (2005) Presynaptic Na^+ channels: locus, development and recovery from inactivation at a high-fidelity synapse. J Neurosci 25:3724–3738.

Lee SH, Rosenmund C, Schwaller B, Neher E (2000) Differences in Ca^{2+} buffering properties between excitatory and inhibitory hippocampal neurons from the rat. J Physiol (Lond) 525:405–418.

Lee SH, Kim MH, Park KH, Earm YE, Ho WK (2002) K^+-dependent Na^+/Ca^{2+} exchanger is a major Ca^{2+} clearance mechanism in axon terminals of rat neurohypophysis. J Neurosci 22:6891–6899.

Morgans CW, El Far O, Berntson A, Wassle H, Taylor WR (1998) Calcium extrusion from mammalian photoreceptor terminals. J Neurosci 18:2467–2474.

Neher E, Augustine GJ (1992) Calcium gradients and buffers in bovine chromaffin cells. J Physiol (Lond) 450:273–301.

Oertel D (1999) The role of timing in the brain stem auditory nuclei of vertebrates. Annu Rev Physiol 61:497–519.

Peng Y-Y (1998) Effects of mitochondrion on calcium transients at intact presynaptic terminals depend on frequency of nerve firing. J Neurophysiol 80:186–195.

Regehr WG (1997) Interplay between sodium and calcium dynamics in granule cell presynaptic terminals. Biophys J 73:2476–2488.

Regehr WG, Delany KR, Tank DW (1994) The role of presynaptic calcium in short-term enhancement at the hippocampal mossy fiber synapse. J Neurosci 14:523–537.

Reuter H, Porzig H (1995) Localization and functional significance of the Na^+/Ca^{2+} exchanger in presynaptic boutons of hippocampal cells in culture. Neuron 15:1077–1084.

Sanchez-Armass S, Blaustein MP (1987) Role of sodium-calcium exchange in regulation of intracellular calcium in nerve terminals. Am J Physiol 252:C595–C603.

Sätzler K, Soehl LF, Bollmann JH, Borst JG, Frotscher M, Sakmann B, Luebke JHR (2002) Three-dimensional reconstruction of a calyx of Held and its postsynaptic principal neuron in the medial nucleus of the trapezoid body. J Neurosci 22:10567–10579.

Schneggenburger R, Neher E (2000) Intracellular calcium dependence of transmitter release rates at a fast central synapse. Nature 406:889–893.

Suzuki S, Osanai M, Mitsumoto N, Akita T, Narita K, Kijima H, Kuba K (2002) Ca^{2+}-dependent clearance via mitochondrial uptake and plasmalemmal extrusion in frog motor nerve terminals. J Neurophysiol 87:1816–1823.

Tang Y, Zucker RS (1997) Mitochondrial involvement in post-tetanic potentiation of synaptic transmission. Neuron 18:483–491.

Taschenberger H, von Gersdorff H (2000) Fine-tuning an auditory synapse for speed and fidelity: developmental changes in presynaptic waveform, EPSC kinetics, and synaptic plasticity. J Neurosci 20:9162–9173.

von Gersdorff H, Borst JG (2002) Short-term plasticity at the calyx of Held. Nat Rev Neurosci 3:53–64.

Wu SH, Kelly JB (1993) Response of neurons in the lateral superior olive and medial nucleus of the trapezoid body to repetitive stimulation: intracellular and extracellular recordings from the mouse brain slice. Hear Res 68:189–201.

Zenisek D, Matthews G (2000) The role of mitochondria in presynaptic calcium handling at a ribbon synapse. Neuron 25:229–237.

Zhong N, Beaumont V, Zucker RS (2001) Roles for mitochondrial and reverse mode Na^+/Ca^{2+} exchange and the plasmalemma Ca^{2+} ATPase in post-tetanic potentiation at crayfish neuromuscular junctions. J Neurosci 21:9598–9607.

Zhou Z, Neher E (1993) Mobile and immobile calcium buffers in bovine adrenal chromaffin cells. J Physiol (Lond) 469:245–273.